PHILOSOPHICAL TRANSACTIONS OF THE ROYAL SOCIETY A MATHEMATICAL, PHYSICAL & ENGINEERING SCIENCES

The growth and characterization of a-sexithienyl–based light–emitting diodes

R. N. Marks, F. Biscarini, T. Virgili, M. Muccini, R. Zamboni and C. Taliani

Phil. Trans. R. Soc. Lond. A 1997 **355**, 763-773
doi: 10.1098/rsta.1997.0042

The growth and characterization of α-sexithienyl-based light-emitting diodes

By R. N. Marks, F. Biscarini, T. Virgili, M. Muccini, R. Zamboni and C. Taliani

Istituto di Spettroscopia Molecolare, Consiglio Nazionale delle Ricerche, Via P. Gobetti 101, 40129 Bologna, Italy

We describe the mechanisms of growth of sublimed thin films of α-sexithienyl and how the morphology of the films can be controlled by using different growth conditions and substrates. The molecules of α-T6 prefer to stand upright on the substrate surface if possible, forming a highly ordered film, and we find that partially polarized photoluminescence and electroluminescence is possible from these films provided that energy migration to randomly oriented defect sites is properly controlled.

We have also investigated the effects of a SiO interfacial layer at the interface between α-T6 and the aluminium negative contact in light-emitting diodes grown in ultra-high vacuum. This is expected to alter the injection properties of electrons into the diodes, which should modify the electroluminescent efficiency. The efficiency is a strong function of the SiO thickness, and the optimum thickness lies at about 2 nm of SiO, which is a reasonable figure for the expected mechanism of electron tunnelling across the barrier. The current–voltage curves are thermally activated and we find that they are also strongly affected by the thickness of this interfacial layer. As the thickness increases from 1–4 nm, the voltage required to drive the light-emitting diode at 0.5 mA drops by about an order of magnitude. from about 15–2 V. The reason for this drop in drive voltage is not yet clear.

1. Introduction

We have made light-emitting diodes (LEDs) in high vacuum and ultra-high vacuum based on thin films of α-sexithienyl (α-T6), in order to study the fundamental processes of charge and energy transport in organic LEDs. We chose to use α-T6 because it is a very well characterized material, even though its fluorescence efficiency is too low to make it of interest in a commercial LED application.

The structure and molecular orientation in films of α-T6 depends primarily on the type of substrate, its temperature and the rate of growth. On polar substrates the molecules prefer to stand upright on the surface at an angle of about 30° to the surface normal in a characteristic herringbone pattern (Ostoja *et al.* 1993; Servet *et al.* 1993; Porzio *et al.* 1993*a*; Porzio *et al.* 1993*b*). With the substrate at room temperature, and with a sufficiently low growth rate, a sublimed film retains much of the structure of the single crystal, which belongs to the $P21/n$ space group (Horowitz *et al.* 1995). As the growth temperature increases the degree of ordering increases (Servet *et al.* 1994; Hamano *et al.* 1994), and in films of 100 nm on mica the lateral size of the grains grows exponentially with substrate temperature from 0.033 μm^2 (at 25 °C) to

Phil. Trans. R. Soc. Lond. A (1997) **355**, 763–773
Printed in Great Britain

1.6 μm^2 (150 °C), while above 200 °C the film is made of large anisotropic lamellae (Biscarini *et al.* 1995). The particle size distributions show that the grains grow by coalescence of small domains in favour of larger ones, a process which is usually controlled by the diffusion of molecules or clusters at inter-grain contacts in such a way as to minimize the surface energy of the joint. From a statistical analysis of the particle sizes, we have extracted the growth activation energy to be 0.36 ± 0.04 eV (Biscarini *et al.* 1995). This is in excellent agreement with the calculated corrugation of the Van der Waals potential that is experienced by a T6 molecule diffusing on a surface of T6 molecules.

The electronic properties of α-T6 are also well characterized, particularly from field effect transistor measurements (Garnier *et al.* 1990; Ostoja *et al.* 1993; Servet *et al.* 1994; Dodabalapur *et al.* 1995; Torsi *et al.* 1996) and this material has the highest hole mobility of any organic material so far discovered in thin film form, of 2×10^{-2} cm^2 Vs^{-1}. The conductivity is highest within the plane of a sublimed film, since the overlap between two molecules lying side-by-side is higher than for molecules lying end-to-end. In the single crystal the hole mobility is 0.5×10^{-2} cm^2 Vs^{-1} (Horowitz *et al.* 1996).

We have studied the growth mechanisms of α-T6 films, from the first few monolayers onwards, using scanning force microscopy (SFM), and we discuss how the structure of films can be controlled by using different growth conditions. We have explored the effect of the substrate temperature during deposition (between 25 and 275 °C) and that of the amount of deposited material (from submonolayer coverage to 300 nm thickness). The lowest lying optical transition in α-T6 is aligned parallel to the molecular axis (Lazzaroni *et al.* 1991; Dippel *et al.* 1993) and we show how the molecular orientation in thin films can lead to anisotropic and partially polarized emission from α-T6-based LEDs provided that energy migration is sufficiently well controlled (Marks *et al.* 1995). We have also studied the effects of the Al–α-T6 interface in LEDs using diodes grown in UHV, in which we have placed a thin spacer layer of SiO between the α-T6 and metal. This allows us to study charge transport across a clean interface with a known structure.

2. Experimental

For the SFM measurements, films were grown on ruby mica because the extremely small roughness of this substrate does not mask the intrinsic features of the film. Films were grown by sublimation in high vacuum (10^{-6}–10^{-7} mbar). The deposition rates (0.02–0.11 nm s^{-1}) were monitored by a quartz oscillator and kept constant within the limits of experimental error. The samples were imaged by a Topometrix 2010 SFM operated in contact mode. Soft cantilevers (0.06 N m^{-1}) and a dry N_2 atmosphere were used in order to minimize possible sample damage. Load forces were estimated to be in the range 1–10 nN.

For measurements of polarized emission LEDs were grown in high vacuum at about 0.1–0.2 nm s^{-1} rate on substrates of glass–ITO. 150 nm films were grown at substrate temperatures between room temperature and 150 °C to control the film morphology, giving average grain diameters within the film ranging between about 200 nm and 1.5 μm. The top contact was made with aluminium, which formed the negative contact. We estimate the external quantum efficiency of these diodes to be about 0.001%. We detected polarized emission by measuring the angular dependence of photoluminescence and electroluminescence in the same samples (discussed later).

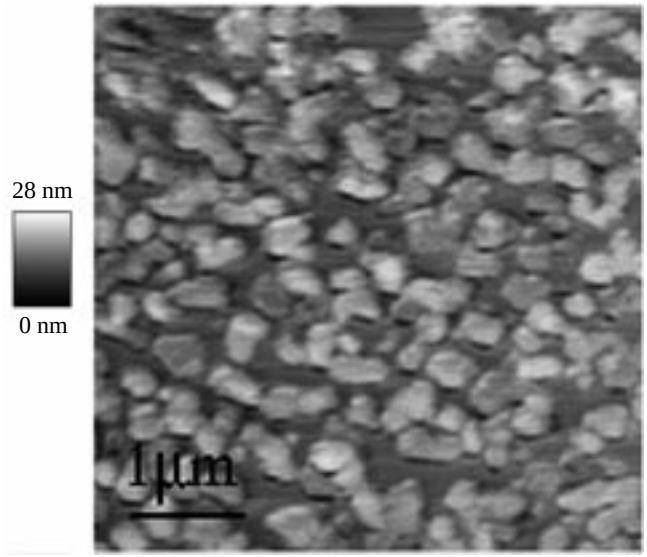

Figure 1. 5 μm × 5 μm SFM image of α-T6 islands (lighter features) grown on mica at 25 °C. The resolution is 200 × 200 pixels. The mean film thickness is about 10 nm.

In the former, films were excited with 514 nm radiation from an argon-ion laser. The sample was held fixed and luminescence was collected with a fibre-optic bundle that was moved around the sample in a semicircle with a polarizer in front to select the desired polarization of light. Electroluminescence measurements were made instead by rotating the sample, which was masked at the edges to prevent collection of waveguided light.

For the UHV experiments, 150 nm films of α-T6 were grown by organic molecular beam deposition at a rate of 0.01–0.02 nm s^{-1}. The base pressure of the system was 3×10^{-10} mbar, and the pressure during deposition was 1×10^{-9} mbar. A film of SiO was deposited on the sample by thermal evaporation with a thickness between 1 and 4 nm, before evaporation of the aluminium top contact. The thickness of the SiO was calibrated by measuring films grown on mica, even so it is very difficult to give a precise value for the thickness of these films on α-T6. We expect the sticking coefficient of SiO on mica and on α-T6 to be different, and for films of the order of a few monolayers, this could make a significant difference to the total thickness of the film actually deposited. In addition, the surface of α-T6 is not atomically smooth and it is possible that island growth of SiO could occur.

3. Results and discussion

(*a*) *Growth and morphology of α-T6 films*

Figure 1 shows the morphology of very thin film grown with the substrate at 25 °C. The film is discontinuous and is formed by flat islands with irregular shapes. We estimate the mean height of each island to be about 15 nm, which is six or seven monolayers of α-T6 (the height of each terrace is 2.3 nm). The island height–diameter ratio is of the order of 0.01, which suggests two-dimensional growth at this stage. As the coverage increases, the film becomes continuous and formed by small grains (figure 2*a*) whose size increases with the film thickness (figures 2*b–d*). The morphology in figure 2 is typical of three-dimensional growth and by the rounded

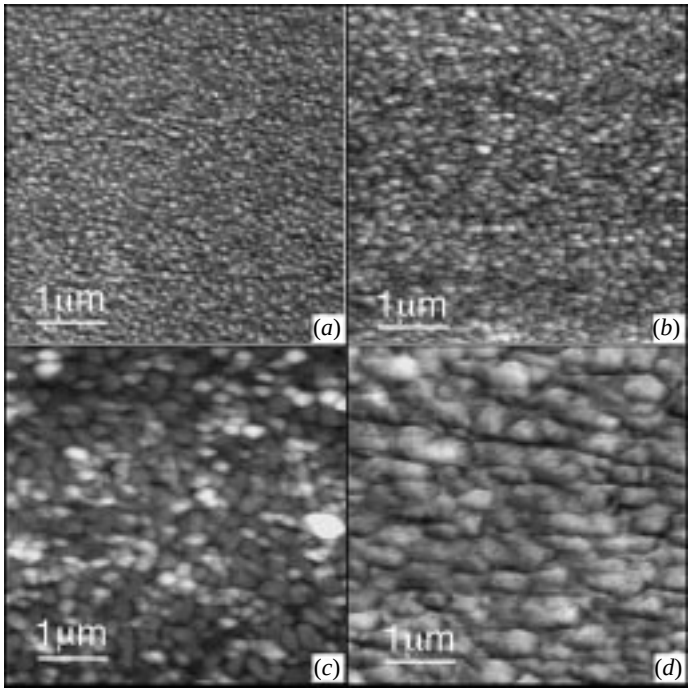

Figure 2. 5 μm × 5 μm SFM images of the morphology of α-T6 films grown on mica at 25 °C for different film thicknesses: (*a*) 12 nm film (height range of image 14 nm); (*b*) 100 nm film (height range 31 nm); (*c*) 325 nm film (height range 81 nm); (*d*) 700 nm film (height range 110 nm).

shape of the grains we can infer that no ordering has built up, so the domains are mostly isotropic.

The growth of films at 150 °C is remarkably different. At submonolayer coverage, crystalline nuclei are formed (figure 3*a*) and their shape suggests that the contact plane with the substrate is the bc crystal plane (Horowitz *et al.* 1995). Nuclei form in rows parallel to cleaved mica terraces and this spatial arrangement induces a preferential orientation in the lamellae seen in films grown at high temperature (Biscarini *et al.* 1995). At 3 nm coverage, which is about one monolayer (figure 3*b*), large branched islands are formed and their shape is reminiscent of the structures typically generated by a diffusion-limited process. The average height of the islands with respect to the background is 6 nm, and 2–3 nm terraces are also resolved. Thus, each island is formed by two molecular layers with T6 molecules standing approximately upright. In the regions where islands have coalesced the aggregates they form still contain a large number of voids, in agreement with a large diffusional barrier for movement of α-T6 molecules. In comparison to figure 1, the much lower density of islands is a consequence of the tendency of the nuclei to form mainly at substrate defects under high temperature growth conditions. Even at 5 nm (two monolayer coverage) the film is not yet continuous and 6–7 nm deep cracks separate large islands (figure 3*c*). On top of the large islands, there are regularly-shaped terraces whose average step is 2.3 ± 0.4 nm, in excellent agreement with the 2.4 nm interlayer spacing from crystallographic data (Horowitz *et al.* 1995). This is clear evidence of a layer-by-layer growth which continues in films up to at least 50 nm (figure 3*d*). At this coverage, new islands sprout off the domain boundaries, as a secondary nucleation, and they appear to coalesce into elongated domains which eventually lead to the formation of

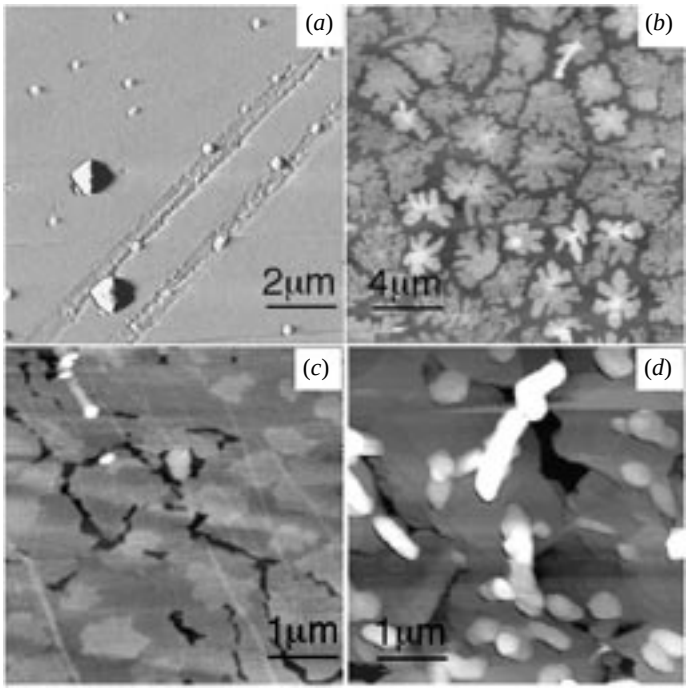

Figure 3. Growth of α-T6 film on mica at 150 °C for different film thickness. (*a*) 1 nm film (less than one monolayer); nuclei anchored at mica cleavage planes. The image has been shaded from the left. (*b*) 3 nm film (one monolayer): highly branched islands. Height range 28 nm. (*c*) 5 nm film (two monolayers): mono-molecular terraces on large T6 islands. Height range 22 nm. (*d*) 50 nm film(25 monolayers): secondary nucleation at T6 film grain boundaries. Height range 36 nm.

lamellae (Biscarini *et al.* 1995) in place of isotropic grains. The secondary nucleation might arise from the necessity to release the stress produced by an ordered layer-by-layer growth with constraints. We are in the progress of investigating whether there is a breakdown of the ordered growth for large thickness.

(*b*) *Polarized electroluminescence in LEDs based on α-T6*

In most conjugated organic materials electroluminescence and photoluminescence arise from the emission of light from a rigid-rod molecule or segment of a polymer chain in which the lowest electronic excited state is polarized along the long molecular axis. Although light may be emitted with a particular polarization with respect to each emitting dipole, the dipoles are generally isotropically distributed, giving rise to an average emission that is unpolarized and isotropic. As we have discussed above, α-T6 films are highly ordered, and thus we expect to be able to see the anisotropic emission of light from each individual molecule in terms of a bulk anisotropy of the luminescence together with partially polarized emission.

We have used the angular dependence of luminescence from α-T6 films to measure the anisotropy of emission, as shown in figure 4. The measured angular dependence is determined both by the distribution of emission within the film and the effects of refraction and reflection at the film surface. For isotropic emission within the film, the latter effect generates an approximately cosine-type dependence of the intensity on θ (Greenham *et al.* 1994). In contrast, for films of α-T6 we expect the internal emission distribution to be highly anisotropic. For the *p*-polarized light, the max-

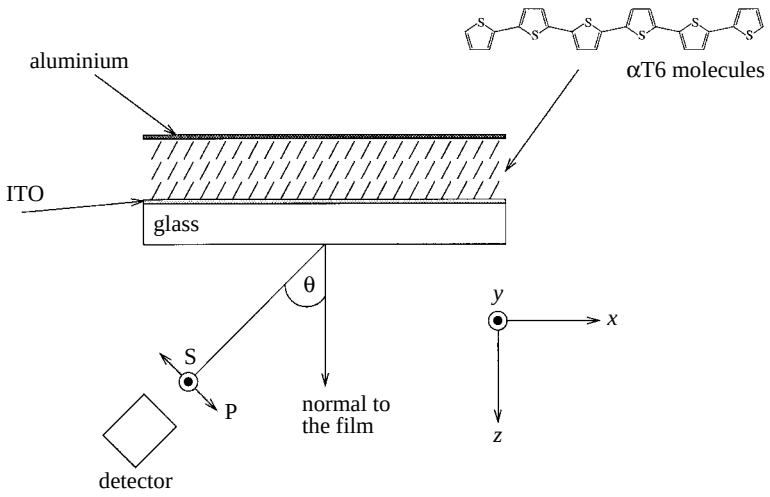

Figure 4. Sketch of a LED and the method of measuring the angular dependence of light emission. The angle θ can be varied between -90 and $+90^\circ$ in the x–z-plane. The intensity of the s-polarized and p-polarized emission (marked on the figure) is measured using a polarizer before the detector.

imum intensity of emission within the film is at high viewing angles, since light is emitted perpendicular to the axis of the dipoles. The measured distribution is then determined by a competition between the internal emission distribution and the effects of reflection and refraction, giving lobes in the emission at some angle from the normal to the film. The s-polarized light is uniformly distributed inside the film, since the net dipole moment for this polarization is parallel to the y-axis in figure 4, and therefore independent of the viewing angle. Externally, the s-polarized component has just a cosine-type dependence on θ.

The dependence of luminescence anisotropy on the film morphology can be interpreted in terms of exciton migration to randomly oriented defect sites in the film. Films made at low temperature have a higher concentration of defect sites and grain boundaries and therefore it will be much easier for an exciton to find such a trap during its lifetime. In electroluminescence, excitons are created by the recombination of electrons and holes injected form the opposite contacts, and it may be that excitons are created close to defect sites due to the trapping of charge prior to exciton formation. The importance of this latter effect can be determined by measuring the angular dependence of photoluminescence in which excitons can be created uniformly throughout the film by the incident light.

Figure 5*a* shows the angular dependence of electroluminescence in diodes made at temperatures of 22 °C (*ca.* 200 nm grain diameter) 104 °C (*ca.* 600 nm diameter) and 155 °C (*ca.* 1500 nm diameter). Luminescence from the film grown at room temperature is completely unpolarized, even though X-ray measurements show that such films are well ordered. A small amount of anisotropy can be seen, however, in the luminescence of the film made at 104 °C, and there are very clear lobes visible in that of the film made at 155 °C, consistent with what we would expect from the bulk morphology of the films.

Figure 5*b* shows this photoluminescence measured on the same films as were used for the electroluminescence experiments (using a clear patch of α-T6 on the ITO sub-

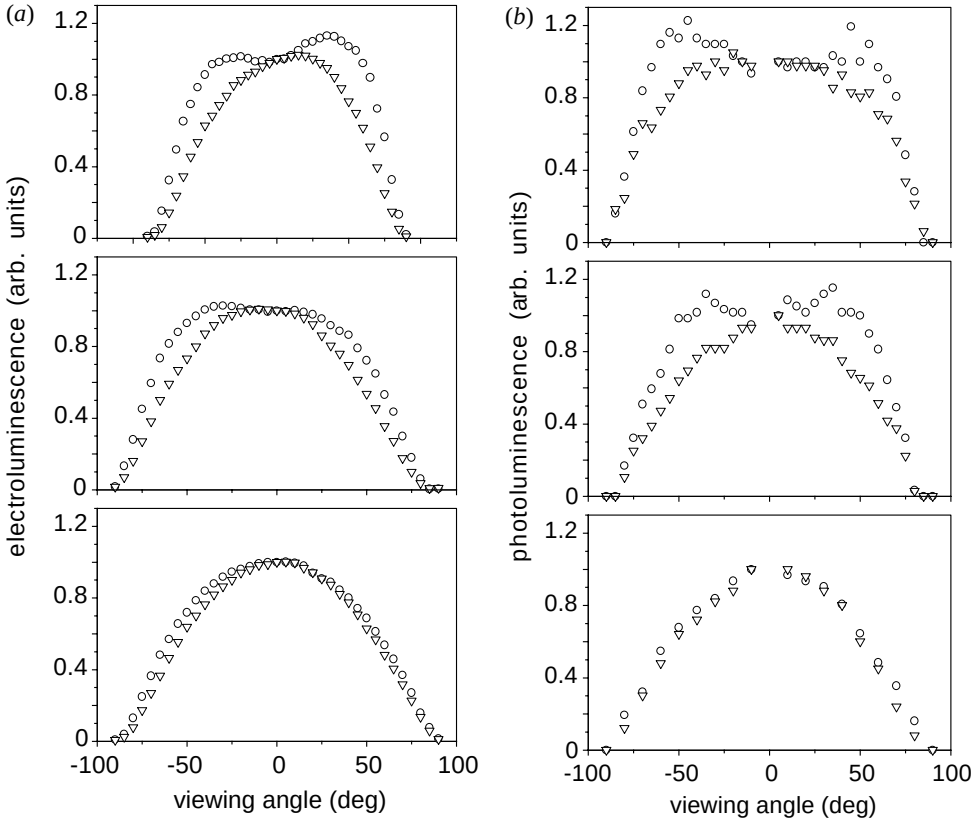

Figure 5. (*a*) The angular dependence of electroluminescence in α-T6–based LEDs for devices made at 155 °C (top), 104 °C (centre), and 55 °C (bottom) substrate temperature. (*b*) The angular dependence of photoluminescence in the same samples. In both figures ▽ represents the *s*-polarized light, ○ represents the *p*-polarized light.

strate). The photoluminescence is isotropic in the film made at 22 °C, but is similar to the electroluminescence for the 104 and 155 °C samples. This clearly illustrates that for films made at room temperature exciton migration alone is sufficient to prevent polarized emission. For the film made at 104 °C the polarization seen in photoluminescence is greater than for electroluminescence, and this may be due to the different spatial positions in which excitons are created in the two different experiments.

(*c*) *The role of the α-T6–Al interface in LEDs*

Recent attempts to make LEDs from α-T6 and other materials in UHV have shown that diodes made in such a clean environment can have a much lower efficiency than diodes made in the more usual 'dirty' environment (Bröms *et al.* 1995). This was interpreted in terms of the behaviour of the organic–metal interface which was presumed to be more efficient at injecting electrons into the organic material when there was a degree of contamination. This hypothesis was tested by evaporating the aluminium top contact in a partial pressure of oxygen ranging from 10^{-10} mbar to about 10^{-5} mbar. The optimum device performance was found at a partial pressure of oxygen of around 10^{-6} mbar in the vacuum system used.

It has been found that the interface between organic materials and metals is com-

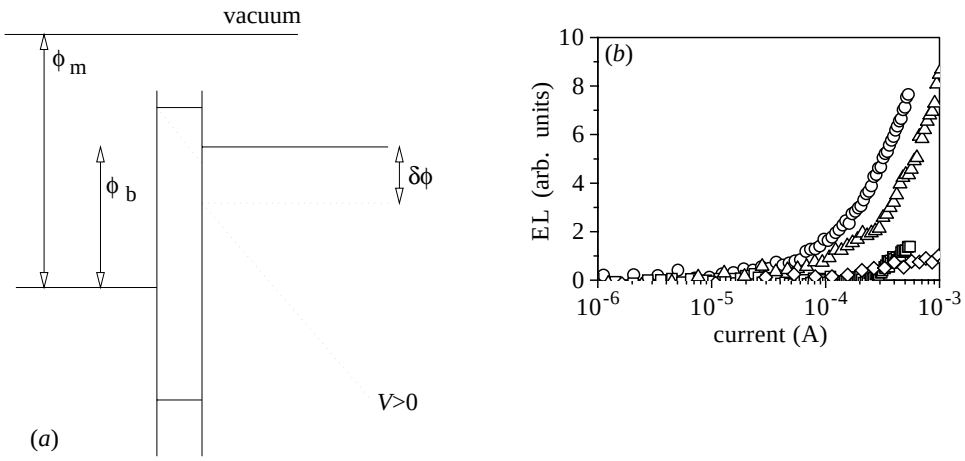

Figure 6. (*a*) The effect of an interfacial layer on the barrier height. With no voltage (solid lines) the barrier height is ϕ_{b} (ϕ_{m} is the metal work function). With V applied, the voltage drop across the insulator lowers the semiconductor band by $\delta\phi$ with respect to the metal Fermi level. (*b*) The luminescence versus current as a function of the SiO thickness (legend: □, 1 nm SiO; ○, 2 nm SiO; △, 3 nm SiO; ◇, 4 nm SiO.)

plex and in all the systems tested so far some form of chemical reaction or doping occurs which probably modifies strongly the electronic properties of the interface (Salaneck & Bredas 1996). Aluminium tends to form covalent bonds with conjugated molecules, breaking the conjugation in the process. When oxygen is present in the chamber during evaporation, the most probable effect is that a layer of aluminium oxide forms on the organic surface before clean metal is laid down. This will both add a barrier between the metal and the organic layer and modify the chemical reaction at the interface.

It has been well known for several decades that an interfacial layer between a metal and a semiconductor can alter the ratio of injection of electrons and holes across the barrier (Card & Rhoderick 1971, 1973; Rhoderick & Williams 1988) and so we have attempted to quantify the effects of a barrier layer at the interface between aluminium and α-T6 in LEDs grown in UHV. The mechanism by which electron injection may be increased in shown in figure 6*a*. On application of an applied field there is a voltage drop across the spacer layer which lowers the LUMO of the α-T6 with respect to the Fermi level of the metal. This effect tends to increase the tunnelling current, in competition with the width of the spacer layer, which tends to decrease the current. In general we expect a balance between these two effects, resulting in a peak in the electron injection (and thus electroluminescent efficiency) at a barrier thickness of the order of a few nm.

Figure 6*b* shows curves of electroluminescence versus current flow for four diodes with different thicknesses of the SiO spacer layer. As this thickness increases, the efficiency first rises and then falls again. The diode with 2 nm of SiO is about eight times more efficient than the diode with 1 nm of SiO. There are not enough curves to assign an optimum SiO thickness, but the efficiency clearly peaks in the region of around 2 nm that we would expect from a process of tunnelling of electrons through the SiO. By the time the thickness reaches 4 nm the layer is already too thick for

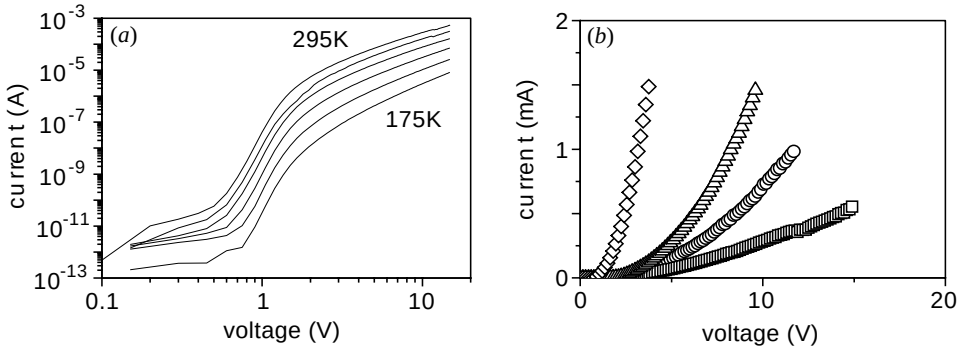

Figure 7. (*a*) The current–voltage curve of a diode with 1 nm of SiO as a function of temperature. In the electroluminescent regime the current flow is thermally activated, with $E_a \sim 0.07$ eV. (*b*) Current–voltage curves of diodes as a function of SiO thickness. (legend: □, 1 nm SiO; ○, 2 nm SiO; △, 3 nm SiO; ◊, 4 nm SiO.)

efficient tunnelling of electrons and the efficiency is lower than in the diode with only 1 nm of SiO.

Figure 7*a* shows current voltage (I–V) curves for a diode with 1 nm of SiO between the α-T6 and metal as a function of temperature. All the I–V curves measured have a similar dependence on temperature, which shows that the current is limited by a thermally activated process. Figure 7*b* shows I–V curves taken at room temperature as a function of the thickness of the SiO barrier layer. The voltage required to attain a current of 0.5 mA drops by an order of magnitude as the SiO thickness is increased from 1 nm to 4 nm. In comparison, the voltage required to drive a α-T6-based LED made in high vacuum (*ca.* 10^{-6} mbar) is similar to the 4 nm curve. For thermionic emission across an interfacial layer between two metal electrodes the current should drop, for a fixed field, as the thickness of the layer increases (Simmons 1964). In our diodes the opposite happens, and although there is no clear explanation for this yet we expect that the chemical reaction between aluminium and α-T6 is important here. In the case of Al–α-T6 junctions evaporating, a layer of SiO does not simply add an interfacial layer, it also prevents the formation of a different layer caused by the chemistry of the interface.

4. Conclusions

Our study of the growth of α-T6 films shows that a large variety of film morphology can be obtained by varying deposition temperature and film thickness, and orientation of the domains can be induced by the underlying substrate. In the case of mica, the dominant contact plane corresponds to molecules standing upright with respect to the substrate. Furthermore, large anisotropic domains can be obtained along the main crystallographic directions obtaind by cleavage of the substrate, which suggests that a suitable choice of substrate (for instance a reconstructed metal or semiconductor surface) could be used to tailor the properties of these films.

This control of the morphology of α-T6 films makes it possible to fabricate LEDs which emit partially polarized light. The most important aspect is control of energy migration within the emissive material. When the defect density is too high, emission from defect sites (both at grain boundaries and within the grains) dominates the fluorescence. In the present configuration most light is emitted sideways, and is

therefore lost, but with a greater understanding of the growth mechanisms of sublimed organic films it may be possible to achieve polarized electroluminescence from molecules that lie flat on the substrate.

The properties of α-T6-based LEDs are mostly determined by the electrical properties of their interfaces. We have found that we can dramatically alter the efficiency of LEDs by using an interfacial layer of SiO between the metal and organic material. An interfacial layer will tend to prevent the chemical reaction that occurs at the interface and with an applied bias this layer alters the positions of the energy levels at the interface giving an optimum thickness of SiO for injection of electrons across the interface of around 2 nm.

This work has been partly supported by the European Commission under the ESPRIT Basic Research program 'LEDFOS'.

References

Biscarini, F., Zamboni, R., Samori, P., Ostoja, P. & Taliani, C. 1995 Growth of conjugated oligomer thin films studied by atomic force microscopy. *Phys. Rev.* B **52**, 14 868–14 877.

Bröms, P., Bitgerson, J., Johansson, N., Lögdlund, M. & Salaneck, W. R. 1995 Calcium electrodes in polymer LEDs. *Synth. Met.* **74**, 179–181.

Card, H. C. & Rhoderick, E. H. 1971 Studies of tunnel MOS diodes. *J. Phys.* D **4**, 1589–1611.

Card, H. C. & Rhoderick, E. H. 1973 The effect of an interfacial layer on minority carrier injection in forward-biased silicon Schottky diodes. *Solid State Electron.* **16**, 365–374.

Dippel, O., Brandl, V., Bässler, H., Danieli, R., Zamboni, R. & Taliani, C. 1993 Energy-dependent branching between fluorescence and singlet exciton dissociation in sexithienyl thin films. *Chem. Phys. Lett.* **216**, 418–423.

Dodabalapur, A., Torsi, L. & Katz, H. E. 1995 Organic transistors: two-dimensional transport and improved electrical characteristics. *Science* **268**, 270–271.

Garnier, F., Horowitz, G., Peng, X. & Fichou, D. 1990 An all-organic soft thin-film transistor with very high carrier mobility. *Adv. Mater.* **2**, 592–594.

Greenham, N. C., Friend, R. H. & Bradley, D. D. C. 1994 Angular dependence of the emission from a conjugated polymer light-emitting diode—implications for efficiency calculations *Adv. Mater.* **6**, 491–494.

Hamano, K., Kurata, T., Kubota, S. & Koezuka, H. 1994 Organic molecular beam depostion of α-sexithienyl. *Jpn. J. Appl. Phys.* B **33**, 1031–1034.

Horowitz, G., Bachet, B., Yassar, A., Lang, P., Demanze, F., Fave, J.-L. & Garnier, F. 1995 Growth and characterisation of sexithiophene single crystals. *Chem. Mater.* **7**, 1337.

Horowitz, G., Garnier, F., Yassar, A., Hajlaoui, R. & Kouki, F. 1995 Field-effect transistor made with a sexithiophene single crystal. *Adv. Mater.* **8**, 52–54.

Lazzaroni, R., Pal, A. J., Rossini, S., Ruani, G., Zamboni, R. & Taliani, C. 1991 Electronic and infrared properties of the α-sexithienyl single crystal. *Synth. Met.* **42**, 2359–2362.

Marks, R. N., Biscarini, F., Zamboni, R. & Taliani, C. 1995 Polarised electroluminescence from vacuum-grown organic light-emitting diodes. *Europhys. Lett.* **32**, 523–528.

Ostoja, P., Guerri, S., Rossini, S., Servidori. M., Taliani, C. & Zamboni, R. 1993 Electrical characteristics of field-effect transistors formed with ordered α-sexithienyl. *Synth. Met.* **54**, 447–452.

Porzio, W., Destri, S., Mascherpa, M. & Brückner, S. 1993*a* Structural aspects of oligothienyl series from X-ray powder diffraction data. *Acta Polymer.* **44**, 266–272

Porzio, W., Destri, S., Mascherpa, M., Rossini, S. & Brückner, S. 1993*b* Structural aspects of oligothienyl series from X-ray powder diffraction data. *Synth. Met.* **55–57**, 408–413.

Rhoderick, E. H. & Williams, R. H. 1988 *Metal–semiconductor contacts*, 2nd edn. Oxford: Clarendon.

Salaneck, W. R. & Bredas, J.-L. 1996 The metal-on-polymer interface in polymer light-emitting diodes. *Adv. Mater.* **8**, 48–54.

Servet, B., Ries, S., Trotel, M., Alnot, P., Horowitz, G. & Garnier, F. 1993 X-ray determination of the crystal structure and orientation of vacuum evaporated sexithiophene films. *Adv. Mater.* **5**, 461–464.

Servet, D., Horowitz, G., Ries, S., Lagorsse, O., Alnot, P., Yassar, A., Deloffre, F., Srivastava, P., Hajlaoui, R., Lang, P. & Garnier, F. 1994 Polymorphism and charge transport in vacuum-evaporated sexithiophene films. *Chem. Mater.* **6**, 1809–1815.

Simmons J. G. 1964 Potential barriers and emission-limited current flow between closely spaced parallel metal electrodes. *J. Appl. Phys.* **35**, 2472–2481.

Torsi, L., Dodabalapur, A., Rothberg, L. J., Fung, A. W. P. & Katz, H. E. 1996 Intrinsic transport properties and performance limits of organic field-effect transistors. *Science* **272**, 1462–1464.

PHILOSOPHICAL TRANSACTIONS OF THE ROYAL SOCIETY A MATHEMATICAL, PHYSICAL & ENGINEERING SCIENCES